Cellular and Molecular Life Sciences (2020) 77:885–901
https://doi.org/10.1007/s00018-019-03213-2



ORIGINAL ARTICLE

# Purinergic $P2Y_2$ receptors modulate endothelial sprouting

Severin Mühleder[1,2,3] · Christiane Fuchs[2,4,10] · José Basílio[5] · Dorota Szwarc[2,4] · Karoline Pill[1,2] · Krystyna Labuda[1,2] · Paul Slezak[1,2] · Christian Siehs[6] · Johannes Pröll[2,7,11] · Eleni Priglinger[1,2] · Carsten Hoffmann[8] · Wolfgang G. Junger[1,9] · Heinz Redl[1,2] · Wolfgang Holnthoner[1,2]

Received: 27 December 2018 / Revised: 12 June 2019 / Accepted: 28 June 2019 / Published online: 5 July 2019


## Abstract

Purinergic P2 receptors are critical regulators of several functions within the vascular system, including platelet aggregation, vascular inflammation, and vascular tone. However, a role for ATP release and P2Y receptor signalling in angiogenesis remains poorly defined. Here, we demonstrate that blood vessel growth is controlled by $P2Y_2$ receptors. Endothelial sprouting and vascular tube formation were significantly dependent on $P2Y_2$ expression and inhibition of $P2Y_2$ using a selective antagonist blocked microvascular network generation. Mechanistically, overexpression of $P2Y_2$ in endothelial cells induced the expression of the proangiogenic molecules CXCR4, CD34, and angiopoietin-2, while expression of VEGFR-2 was decreased. Interestingly, elevated $P2Y_2$ expression caused constitutive phosphorylation of ERK1/2 and VEGFR-2. However, stimulation of cells with the $P2Y_2$ agonist UTP did not influence sprouting unless $P2Y_2$ was constitutively expressed. Finally, inhibition of VEGFR-2 impaired spontaneous vascular network formation induced by $P2Y_2$ overexpression. Our data suggest that $P2Y_2$ receptors have an essential function in angiogenesis, and that $P2Y_2$ receptors present a therapeutic target to regulate blood vessel growth.

**Keywords** Endothelial · Purinergic · Angiogenesis · $P2Y_2$ · Tip cell · Sprouting

## Introduction

Mammalian cells use intracellular ATP to fuel virtually all biochemical reactions. However, ATP can also be released in a controlled manner, regulating the functions of various cells in the circulatory system including endothelial cells and neutrophils through autocrine and paracrine signaling mechanisms that involve purinergic receptors [1]. ATP and its sequential degradation to ADP, AMP, and adenosine can activate different sets of the 19 known purinergic receptor subtypes [1, 2]. These receptors have different affinities to these nucleotides and nucleosides. The purinergic receptor family includes P1 adenosine receptors that are G protein-coupled receptors (GPCRs), ATP-gated ion channels named P2X, and GPCRs termed P2Y receptors. P2Y

**Electronic supplementary material** The online version of this article (https://doi.org/10.1007/s00018-019-03213-2) contains supplementary material, which is available to authorized users.

✉ Wolfgang Holnthoner
wolfgang.holnthoner@trauma.lbg.ac.at

1 Ludwig Boltzmann Institute for Experimental and Clinical Traumatology, AUVA Research Center, Donaueschingenstrasse 13, 1200 Vienna, Austria

2 Austrian Cluster for Tissue Regeneration, Vienna, Austria

3 Kompetenzzentrum für MechanoBiologie (INTERREG V-A AT-CZ ATCZ133), Vienna, Austria

4 Department Life Science Engineering, University of Applied Sciences Technikum Wien, Vienna, Austria

5 Department of Vascular Biology and Thrombosis Research, Medical University of Vienna, Vienna, Austria

6 Mag. Dipl.-Ing. Dr. Christian Siehs, IT-Services, GLN 9110002040261, Vienna, Austria

7 Center for Medical Research, Johannes Kepler University, Linz, Austria

8 Institut für Molekulare Zellbiologie, CMB-Center for Molecular Biomedicine, Universitätsklinikum Jena, Friedrich-Schiller-Universität, Jena, Germany

9 Department of Surgery, Beth Israel Deaconess Medical Center, Harvard Medical School, Boston 02215, MA, USA

10 Present Address: Wellman Center for Photomedicine, Massachusetts General Hospital, Boston, MA, USA

11 Red Cross Blood Transfusion Service, Linz, Austria

receptors differ in their affinities for ATP, ADP, UTP, UDP, and UDP-glucose [1]. Endothelial cells express several different purinergic receptor subsets, however, little is known about their functional roles in endothelial cell regulation [1, 3]. The $P2Y_2$, $P2Y_1$, $P2Y_{11}$, and $P2X_4$ receptor subtypes are the most abundantly expressed P2 receptor subtypes found in endothelial cells [3]. Among those, only the $G_{q/11}$-coupled receptor $P2Y_2$ has been reported to be implicated in tissue regeneration. $P2Y_2$ receptors have been shown to have a crucial function in the regeneration of epidermal tissue during wound healing [4, 5]. Nevertheless, the underlying mechanisms are unclear and it is unknown if $P2Y_2$ receptors influence dermal blood vessel growth. It has also been suggested that $P2Y_1$ mediates angiogenesis [6], although the agonist used in that study is not selective and can also activate other P2 receptors [7]. Two studies showed that $P2Y_2$ can interact with VEGFR-2 leading to its activation upon stimulation with UTP [8, 9] and results using global knockout mice revealed that $P2Y_2$ mediates collateral vessel formation after ischemia [10]. Furthermore, it was previously shown that the G protein $G_{q/11}$ is required for VEGF-induced angiogenesis [11], however, the receptor responsible for these effects remains unknown. Taken together, it is increasingly apparent that $P2Y_2$ may be among the candidate GPCRs involved, as it couples to $G_{q/11}$ and can interfere with VEGFR-2 signaling via a mechanism involving Src [12–14]. Yet, experimental evidence demonstrating that $P2Y_2$ is a key driver for VEGF-induced angiogenic sprouting has not been provided so far. In this study, we report that modulation of the expression of $P2Y_2$ receptors on endothelial cells promotes endothelial sprouting by stimulating VEGFR-2 receptor signaling and driving endothelial cells towards a proangiogenic phenotype.

## Methods

### Reagents

Chemicals and antibodies used in this study are listed in the supplementary files (Supplementary Table 1). All other reagents are described in the respective section.

### Cell culture

Human placentae and umbilical cords were obtained at term pregnancy during Caesarean sections with written and informed maternal consent and collection approved by a local ethical committee from Upper Austria (Ethikkommission des Landes Oberösterreich, #200). All methods were performed according to the relevant guidelines and regulations of the local ethical board. Until processing, placentae were stored in sterile bags (Websinger) in Ringer solution (Fresenius, Austria). Human umbilical vein endothelial cells (HUVEC) were either isolated as described previously [15] or purchased as a pooled donor batch from Lonza and used at passages 4–9. Mesenchymal stromal cells (MSC) were isolated from adipose tissue obtained from liposuction material as described before [16] and used at passages 2–10. Induced pluripotent stem cell-derived endothelial colony-forming cells (iPSC-ECFC) were obtained from Axolbio (United Kingdom) and used at passage 4–8. All cells were maintained in Endothelial Cell Growth Medium-2 (EGM-2) from Lonza or Promocell consisting of Endothelial Cell Basal Medium (EBM-2) supplemented with 5% fetal calf serum (FCS) and endothelial growth supplements. To determine that all effects occur specifically due to interference with $P2Y_2$ signaling, we controlled for donor, passage, and virus infection and only included cells within one experiment if they were from the same donor, used at the same passage and were retrovirally infected at the same time. All HUVEC data shown were obtained from several independent experiments where at least two different biological donors from at least two different virus infections were used. In total, $P2Y_2$ was overexpressed in cells derived from six donors, while cells from at least two donors were included in selected experiments such as knockdown/inhibition of $P2Y_2$. Normal spheroid sprouting and fibrin matrix assays were performed with $P2Y_2^{OE}$-HUVEC generated from all six donors.

### siRNA-mediated knockdown

Transfection protocols and sequences and a pool of three different siRNAs were used as previously published [14, 17]. siRNAs were purchased from Qiagen. One-third of each siRNA was used in the transfection mix to knockdown $P2Y_2$ in HUVEC.

### Proliferation assay and measurement of extracellular ATP

$5 \times 10^3$ HUVEC were seeded in 96-well plates and left to attach overnight. Then, cells were washed with 1 × PBS and incubated in EBM-2 ± VEGF at a concentration of 50 ng/ml for 48 h. BrdU assay was then performed as described by the manufacturer (Roche).

To measure ATP release, HUVEC were grown in 96-well plates to confluence. Cells were starved for 4 h in EBM-2 + 1% BSA (Sigma) before stimulation with VEGF 50 ng/ml or thrombin at 1 U/ml for 10 min. Supernatants were then transferred into opaque plates and ATP was determined luminometrically as previously described [18].

## Plasmids and retroviral infection of HUVEC

EGFP and mCherry in pLV vectors and pBMN-Z were purchased from Addgene. pcDNA3-EYFP-HIS was purchased from Invitrogen (Thermo Fisher). Plasmids encoding human $P2Y_2$-YFP and human $P2Y_{11}$-YFP were previously described [19]. EGFP and mCherry were subcloned into pBMN after digestion with *Bam*HI and *Sal*I. EYFP-HIS was subcloned into pBMN after digestion with *Bam*HI and *Eco*RI. Both $P2Y_2$-YFP and $P2Y_{11}$-YFP were digested with *Xho*I and blunted before being digested with *Hind*III. pBMN-Z was digested with *Not*I, and blunted and digested with *Hind*III to enable ligation with $P2Y_2$-YFP or $P2Y_{11}$-YFP. Successful subcloning of both constructs was confirmed by sequencing. Retroviral infection was performed as described previously [20]. Briefly, Phoenix ampho cells (a kind gift of Regina Grillari, University of Natural Resources and Life Sciences, Vienna) were cultured in DMEM (high glucose) and 10% FCS. Virus particle generation was performed by transfecting Phoenix ampho cells at 80% confluency using Lipofectamine 2000 or TurboFect (both from Thermo Fisher) according to the manufacturer's instructions. Supernatant containing virus particles was mixed 50:50 with full medium and transferred onto 80% confluent HUVEC and incubated overnight. YFP-HUVEC, GFP-HUVEC, or mCherry-HUVEC were termed as CTRL-HUVEC, while $P2Y_2$-YFP-HUVEC were labeled as $P2Y_2^{OE}$- and $P2Y_{11}$-YFP-HUVEC as $P2Y_{11}^{OE}$-HUVEC, respectively. All cells were then expanded in new flasks and used for subsequent experiments.

## Embedding of cells in fibrin matrices

Fibrin matrices were generated as described previously [20]. Briefly, fibrin gel components (TISSEEL®, Baxter) were prepared by warming frozen fibrinogen to room temperature and diluting 4 U/ml thrombin 1:10 in calcium chloride ($CaCl_2$). Cells, fibrinogen, and thrombin were mixed and pipetted onto prepared coverslips. Gels polymerized at room temperature for 30 min before growth medium with aprotinin was added. The final concentration of fibrinogen used was 2.5 mg/ml, of thrombin 0.2 U/ml, and of aprotinin 100 KIU/ml. Fibrin scaffolds had a volume of 200 µl and contained 500 endothelial cells (250:250 in mosaic assays) and 500 MSC per µl fibrin. If spheroids were embedded in fibrin, the final concentration of fibrinogen was 2.5 mg/ml, of thrombin 1 U/ml, and of aprotinin 100 KIU/ml. For VEGFR-2 inhibition experiments, the selective antagonist Apatinib (YN968D1, MedChemExpress) was reconstituted in DMSO. To block VEGFR-2 in fibrin matrix assays, this antagonist was added to the normal growth medium (EGM-2, Lonza) at 1 µM with every medium change (i.e., every 2–3 days). For $P2Y_2$ inhibition experiments, the selective antagonist AR-C 118925XX (Tocris) was reconstituted in DMSO. With every medium change, this antagonist was added to the growth medium (EGM-2, Promocell) at a concentration of 30 µM, which was previously shown to inhibit $P2Y_2$ function in ECs [14].

## Spheroid sprouting assay

Generation of spheroids and the sprouting assay were performed as described elsewhere [21]. Briefly, methylcellulose medium was prepared by dissolving 0.6 g of autoclaved methylcellulose (Sigma) in 50 ml EBM-2 (Lonza or Promocell). Cell number was adjusted to generate spheroids containing 1000 cells per spheroid. These cells were suspended in 80% EGM-2 and 20% methylcellulose medium and grown in hanging drops overnight. Spheroids were then harvested, centrifuged, and mixed with 80% methylcellulose medium and 20% FCS to avoid sedimentation of spheroids. Rat tail collagen I (Corning) was diluted to 2 mg/ml with water and 10× DMEM high glucose for equilibration. Then, equal amounts of collagen solution and spheroid suspension were mixed and pipetted into pre-warmed wells of a 48-well plate. Alternatively, harvested spheroids were embedded in fibrin matrices as described above. After 1 h of incubation at 37 °C, EBM-2 with or without hVEGF-$A_{165}$ (Peprotech or Evercyte) at a concentration of 50 ng/ml was added on top of collagen gels and samples were incubated overnight before quantification.

## RNA isolation, transcriptome analysis, and RT-PCR

RNA was isolated from confluent cell monolayers using Trizol (Life Technologies) as described previously [22]. Consequently, isolated RNA from two biological replicates was used to produce biotinylated cRNA, and then purified, fragmented, and hybridized to GeneChip Human Genome U133 Plus 2.0 arrays (Affymetrix) as described elsewhere [22]. The resulting .CEL files were summarized in the Affymetrix Console Software (version 1.4.1.46) using the Robust Multi-array Average (RMA) normalization algorithm (3′ Expression Arrays: RMA, log2). Differential expression analysis was performed in ExAtlas, a gene expression meta-analysis tool [23]. For explorative pathway analysis, genes with a fold change of two or higher, in either direction, were analyzed through the use of IPA (QIAGEN Inc.) [24], focusing on endothelial cells. Gene Set Enrichment Analysis (GSEA) was done using the $\log_2$ ratio of classes ($P2Y_2^{OE}$ vs. CTRL) as the ranking metric. Gene sets were taken from the Molecular Signatures Database v5.2 [25]. Figures were generated using Morpheus [26] and ggplot2.

To perform RT-PCR, complementary DNA (cDNA) was synthesized using an EasyScript™ cDNA Synthesis Kit (abmGood). DNA concentration was measured with spectrophotometer (Nanodrop OneC, Thermo Fisher Scientific). cDNA was mixed with reaction buffer, dNTPs, selected primer (Supplementary Table 2), and Hot Start *Taq* DNA Polymerase (all from New England Biolabs). After an initial denaturation step of 95 °C for 30 s, samples were subjected to 30 cycles of 95 °C for 30 s, 55 °C for 60 s, and 68 °C for 60 s. Then, the procedure was terminated by a final extension step of 68 °C for 5 min. The amplified products were mixed with loading buffer (New England Biolabs), loaded into 1% agarose gels containing ethidium bromide, and subjected to electrophoresis.

## Flow cytometry

Cells were detached using Accutase (Sigma), and centrifuged and fixed using 1% formaldehyde on ice for 15 min. To label $P2Y_2$ or to detect total protein levels, cells were washed once and incubated in 1 × permeabilization buffer for 15 min on ice. Then, cells were stained with selected antibodies on ice as described previously [27]. To adequately detect the antibody signal, compensation settings were applied to reduce the background of the YFP fluorescence. Platelets were isolated from whole blood donated by human volunteers according to a standard protocol from Abcam (Isolation of human platelets from whole blood, Abcam). Platelets were fixed and subjected to the same $P2Y_2$ staining procedure as mentioned above. All samples were measured on a Cytoflex flow cytometer (Beckman Coulter) and data were analyzed using FlowJo X 10.0.7.

## Immunoprecipitation and immunoblotting

For immunoprecipitation, cells were grown to confluency in T75 tissue culture flasks. HUVEC were then starved for 4 h in EBM-2 + 1% BSA (Sigma) before stimulation with 100 ng/ml VEGF for 10 min. Cells were then immediately put on ice and lysed in 1 ml PLCLB lysis buffer (150 mM NaCl, 5% glycerol, 1% Triton X-100, 1.5 mM $MgCl_2$, and 50 mM HEPES, pH 7.5) supplemented with 2 mM sodium orthovanadate, and 1 × protease inhibitor mix (Complete Mini, Roche). Cleared lysates were incubated with anti-human VEGFR-2 (clone D5B1, 1:200, Cell Signaling Technology) primary antibody for 2 h. Subsequently, the immunocomplexes were captured using protein G-Sepharose (Abcam). After three washing steps in PLCLB buffer, the proteins were separated in 7% polyacrylamide gels under reducing conditions. After blotting of the proteins to nitrocellulose membranes and blocking of the membranes in 5% nonfat milk, membranes were probed with monoclonal antibodies against VEGFR-2 (clone D5B1, 1:1000, Cell Signaling Technology) or phosphotyrosine (clone 4G10, 1:1000, Merck). After incubation with the secondary anti-rabbit (Acris Antibodies) or anti-mouse (Jackson Immuno Research) HRP-coupled antibodies, respectively, the signal was visualized by chemiluminescence (BioRad). Cell lysis of confluent, unstimulated HUVEC, and processing and immunoblotting of ERK 1/2, p-ERK 1/2, AKT, p-AKT, rS6, and p-rS6 were performed as described elsewhere [18].

## Immunofluorescence staining

Endothelial cells were cultured in borosilicate glass chamber slides (Nunc). Cells were washed with 1 × PBS, fixed with 4% paraformaldehyde for 15 min, and permeabilized using 1 × permeabilization buffer (eBiosciene) for 15 min at room temperature. Cells were then stained with anti-human $P2Y_2$ antibodies (1:200) overnight at 4 °C on a shaker following incubation with anti-rabbit Alexa Fluor 594 antibody (Invitrogen) for 1 h at room temperature. Images were taken on a laser scanning confocal microscope (Zeiss LSM510, Zeiss).

## Quantification of endothelial networks, sprouts, and histological cross sections

Images of endothelial networks in fibrin were taken on an epifluorescence microscope (Zeiss Observer A1) and used for analysis. For network quantification, 3–4 images per sample were taken and analyzed as described previously [20, 27, 28]. Images were processed using Adobe Photoshop CS5 (Adobe Systems) and analyzed in a blinded manner. Measurement of number of tubules, junctions, and total and mean tubule length was done with Angiosys software (TCS Cellworks). To quantify sprouting parameters, z-stacks of spheroids were taken using a Leica DMI6000B microscope at ~ 10 µm intervals to a depth of ~ 200 µm, merged and quantified using ImageJ. All images were randomized and analyzed in a blinded manner.

## Statistics

Statistical evaluations were performed with GraphPad Prism 5 software (GraphPad). Data from spheroid, fibrin matrix assays, and immunoprecipitations were analyzed by two-way ANOVA. siRNA knockdown efficiency was analyzed by paired Student's *t* test. All other data were analyzed by Mann–Whitney test. Values were considered significant when $p < 0.05$.

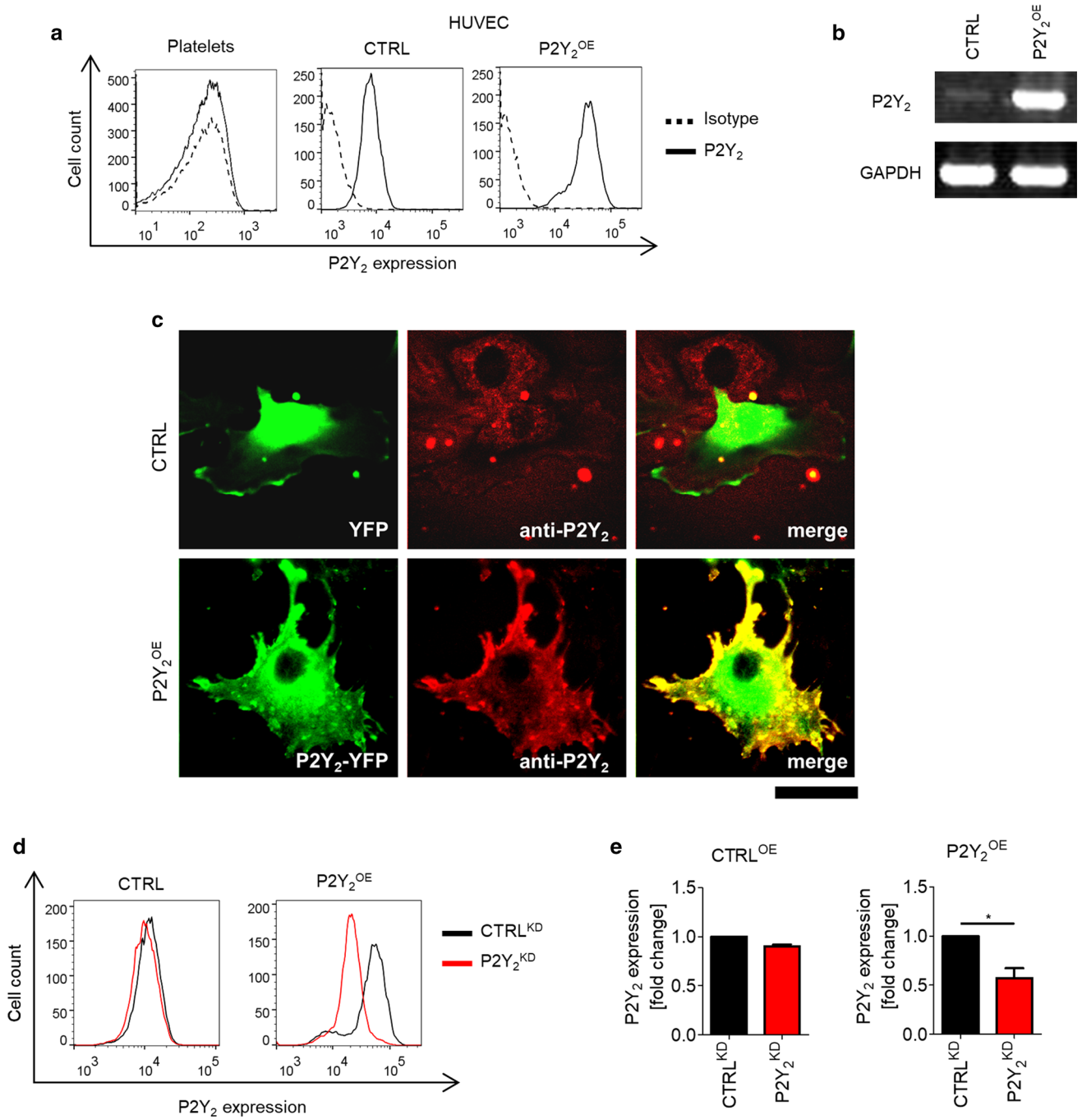


**Fig. 1** Detection of $P2Y_2$ overexpression in HUVEC. **a** Antibody specificity was determined by antibody staining of human platelets, control, and $P2Y_2^{OE}$-HUVEC and detection by flow cytometry. Platelets did not show any expression of $P2Y_2$, while moderate expression was detected on control cells which was increased in $P2Y_2^{OE}$-HUVEC. **b** $P2Y_2$ mRNA was strongly expressed in $P2Y_2^{OE}$-HUVEC compared to controls as determined by RT-PCR. **c** $P2Y_2$-overexpressing and vehicle-infected HUVEC were stained against $P2Y_2$. A strong co-localization of the antibody signal and the $P2Y_2$-fusion protein could be detected in $P2Y_2^{OE}$ cells particularly on cell borders. **d** siRNA-mediated knockdown of $P2Y_2$ reduced $P2Y_2$ protein expression only in $P2Y_2^{OE}$ cells. **e** On average, this resulted in a 10% reduction of protein levels in controls and 47% reduction in $P2Y_2^{OE}$-HUVEC compared to cells transfected with control siRNA. Platelets were isolated from one donor. All other data are representative for three independent experiments conducted with three different HUVEC donors. * indicate a $p$ value of $< 0.05$; scale bar 20 µm

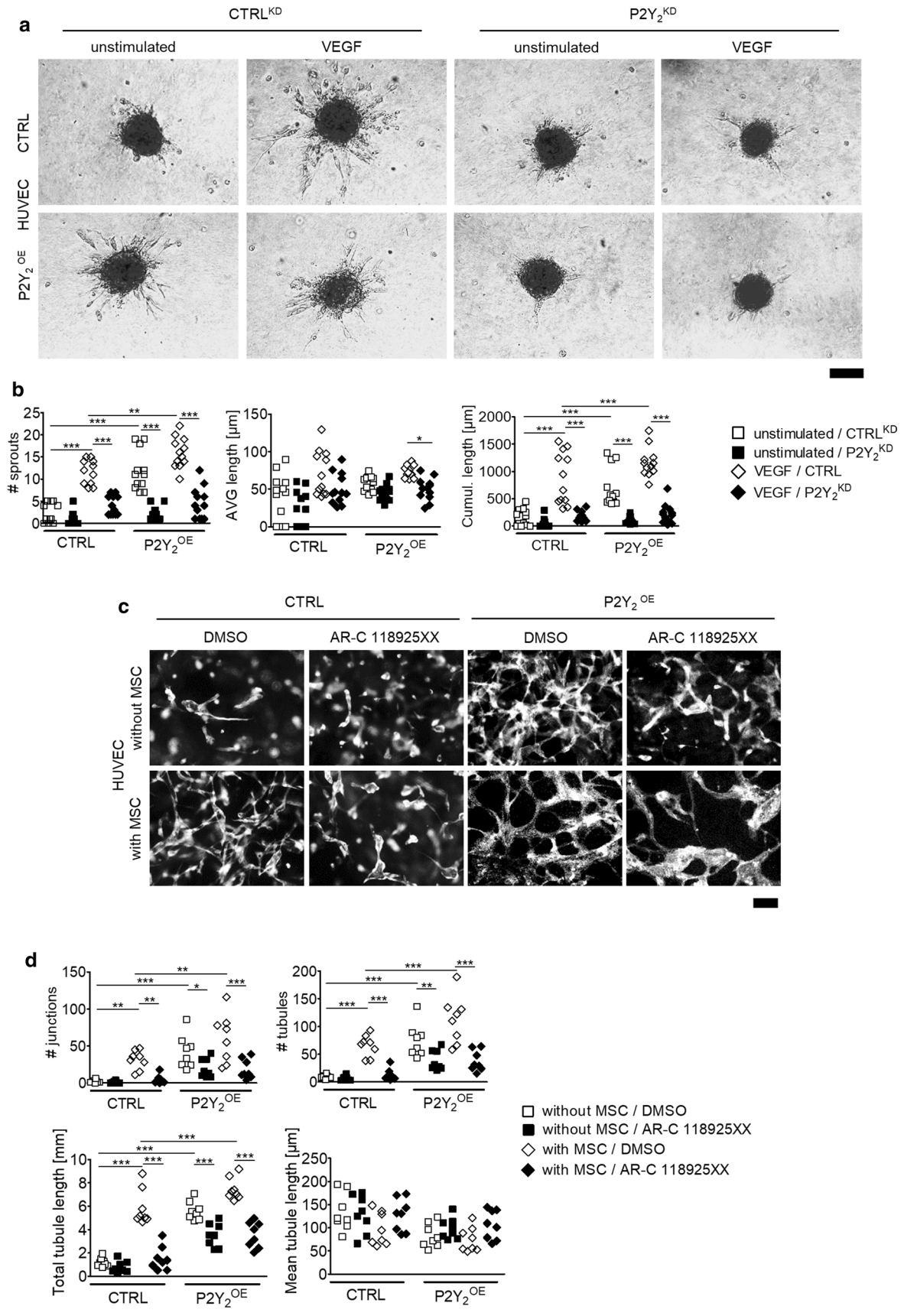
a
CTRL^KD
P2Y2^KD
unstimulated
VEGF
unstimulated
VEGF
CTRL HUVEC
P2Y2 OE
b
# sprouts
AVG length [µm]
Cumul. length [µm]
CTRL
P2Y2^OE
unstimulated / CTRL^KD
unstimulated / P2Y2^KD
VEGF / CTRL
VEGF / P2Y2^KD
c
CTRL
P2Y2 OE
DMSO
AR-C 118925XX
DMSO
AR-C 118925XX
HUVEC without MSC
with MSC
d
# junctions
# tubules
Total tubule length [mm]
Mean tubule length [µm]
CTRL
P2Y2^OE
without MSC / DMSO
without MSC / AR-C 118925XX
with MSC / DMSO
with MSC / AR-C 118925XX

◂**Fig. 2** $P2Y_2$ influences sprouting and vasculogenesis in HUVEC in vitro. **a** Representative images of HUVEC spheroids. $P2Y_2$ overexpression (OE) or knockdown (KD) correlated with sprouting potential independently of VEGF 50 ng/ml addition. **b** Quantitative analysis of spheroids revealed that sprouting behaviour is significantly affected by $P2Y_2$ expression in HUVEC spheroids as determined by the number of sprouts, average length, and cumulative length of sprouts per spheroid. **c** Representative images of HUVEC embedded in fibrin either alone or in co-culture with MSC, showing that enhanced $P2Y_2$ expression or inhibition of $P2Y_2$ by the selective antagonist AR-C 118925XX (30 μM) modulated vasculogenic network formation in fibrin. **d** Analysis of network parameters reveal that $P2Y_2$ is essential for vascular network formation in fibrin. Graphs show data obtained from two independent experiments using two different HUVEC donors *, ** and *** indicate $p$ values of $<0.05$, 0.01, and 0.001, respectively. Scale bars indicate 100 μm

## Results

### Detection of $P2Y_2$ overexpression in HUVEC

To identify the role of $P2Y_2$ in vascular network formation, we overexpressed $P2Y_2$-YFP ($P2Y_2^{OE}$) [19] in human umbilical vein endothelial cells (HUVEC) and measured its expression via flow cytometry and RT-PCR. To confirm the specificity of the antibodies used, a $P2Y_2$ staining and flow cytometric analysis of human platelets, control HUVEC, and $P2Y_2$-overexpressing HUVEC was performed. In agreement with the previous reports, $P2Y_2$ expression on platelets could not be detected [29], while moderate and high expression was detected on control and $P2Y_2^{OE}$-HUVEC, respectively (Fig. 1a). In addition, a strong increase in $P2Y_2$ mRNA could be detected upon $P2Y_2$ overexpression in HUVEC (Fig. 1b). $P2Y_2$-YFP was detected in the cytoplasm, on cell–cell borders and in filopodia of HUVEC cultured in a 3D fibrin matrix as visualized (Supplementary movie 1). Furthermore, staining of cultured endothelial cells with an anti-$P2Y_2$ antibody co-localized with the YFP fluorescence signal further demonstrating the antibody specificity (Fig. 1c). Upon knockdown of $P2Y_2$ ($P2Y_2^{KD}$) using previously published $P2Y_2$ siRNA sequences and transfection protocols [14, 17], $P2Y_2$ protein expression was only reduced in $P2Y_2^{OE}$-cells but not in CTRL cells (Fig. 1d, e), indicating relatively low endogenous $P2Y_2$ turnover rate in ECs [30].

### $P2Y_2$ receptors influence sprouting and vasculogenesis

Modulation of purinergic P2Y receptor expression has previously been shown to greatly influence numerous cell functions including cell differentiation and proliferation [31–33]. To determine if and how $P2Y_2$ expression alters sprouting and vascularization, we induced receptor overexpression and performed siRNA-mediated knockdown in HUVEC and examined the effects of these treatments in spheroid sprouting and fibrin co-culture assays. Neither overexpression nor knockdown of $P2Y_2$ significantly influences the percentage of cells present in the gate used for flow cytometry analysis to determine protein expression, suggesting that cell viability is not affected by any of the above-named procedures (data not shown). Overexpression of $P2Y_2$ resulted in an increase of spontaneous sprouting, however, being independent of additional VEGF. siRNA-mediated knockdown of $P2Y_2$ reversed this effect and also led to impaired sprouting in response to VEGF treatment (Fig. 2a). Quantification of the number of sprouts and their cumulative lengths revealed a dependence of sprouting ability on the expression of $P2Y_2$ (Fig. 2b). No significant difference could be detected in the average length of sprouts upon $P2Y_2$ overexpression. However, knockdown of $P2Y_2$ led to a reduction of the average length in VEGF-treated $P2Y_2^{OE}$-HUVEC (Fig. 2b). These results demonstrate that $P2Y_2$ receptors promote sprouting in endothelial cells and that silencing of $P2Y_2$ receptor signaling impairs sprouting. Since this sprouting assay lacks vascular pericytes and only reflects the initial sprouting events (hours) but not functional vascular network formation (days), we employed a fibrin co-culture model of endothelial cells and mesenchymal stromal cells (MSC) [20, 27] to study how $P2Y_2$ receptors influence vascular network formation. In line with the sprouting assay results, overexpression of $P2Y_2$ in HUVEC induced the formation of a primitive vascular network embedded in a fibrin matrix. This occurred in the absence of supporting cells, an effect that was not observed with CTRL-HUVEC. $P2Y_2$ receptor expression had no discernible effect when HUVEC were co-cultured with MSC. However, vascular network formation was inhibited when cells were cultured in the presence of the selective $P2Y_2$ antagonist AR-C 118925XX (Fig. 2c) that led to significantly reduced numbers of junctions, tubules and total tubule lengths (Fig. 2d). These data indicate that endothelial $P2Y_2$ receptors drive vascular network formation.

### $P2Y_2$ overexpression increases expression of proangiogenic genes

To analyze how $P2Y_2$ overexpression regulates the angiogenic potential of endothelial cells, we performed microarray expression analysis. Differentially expressed genes induced by $P2Y_2$ receptor expression in HUVEC were primarily related to the development and function of the cardiovascular system (Fig. 3a). Many of these genes are directly involved in angiogenesis and vasculogenesis (Fig. 3b). Pathway enrichment analysis using two different databases revealed further evidence for the notion that $P2Y_2$ expression regulates endothelial cell physiology (Sup. Fig. 1a, b). Analysis of genes essential in angiogenesis showed a strong increase in transcription of several proteins that are important for

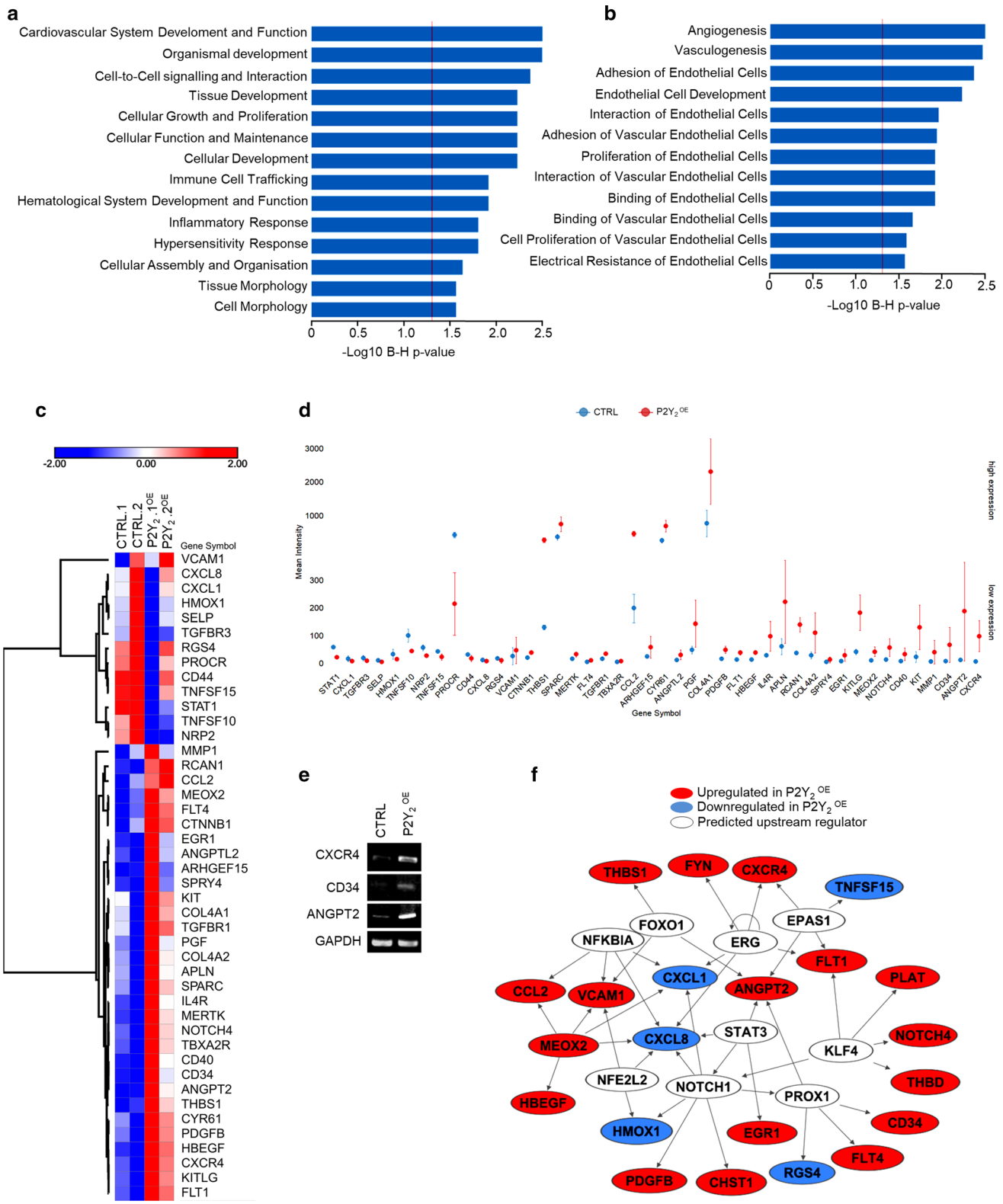


sprouting, including CXCR4, CD34, and ANGPT2 (Fig. 3c). In fact, upon $P2Y_2$ overexpression, transcription of these and other relevant genes was increased by more than ten-fold compared to basal expression (Fig. 3d). In addition, we confirmed the gene array data for CXCR4, CD34, and ANGPT2 using RT-PCR (Fig. 3e). Transcription factor network analysis revealed that NFKBIA, FOXO1, ERG, EPAS1, STAT3, NFE2L2, NOTCH1, KLF4, and PROX1

◂**Fig. 3** Gene array analysis reveals increased expression of proangiogenic genes upon $P2Y_2$ overexpression. **a** IPA-based functional annotation of genes which expression was significantly altered in $P2Y_2^{OE}$-HUVEC, showing that mostly cardiovascular system functions and **b** within this gene set, primarily genes regulating angiogenesis and vasculogenesis were affected by $P2Y_2$ overexpression. **c** Heatmap showing normalized gene expression of these angiogenesis-related genes in two separate donors. A strong increase upon $P2Y_2$ overexpression of CXCR4, CD34, and ANGPT2 could be observed in both donors compared to controls. **d** Mean intensity values of angiogenesis genes demonstrating the strong differences in gene expression in $P2Y_2$-overexpressing cells compared to control cells. CXCR4, CD34, and ANGPT2 showed on average a 10- to 100-fold increase in gene expression. **e** Confirmation of increased gene expression of CXCR4, CD34, and ANGPT2 by RT-PCR. **f** Transcription factor network analysis showing predicted transcriptional upstream regulators based on the gene expression pattern in $P2Y_2$-overexpressing HUVEC. Data were obtained from two different HUVEC donor batches containing pools of three and four donors

are upstream regulators of $P2Y_2$ expression (Fig. 3f), while additional transcription factor targets seem to be enriched in response to $P2Y_2$ overexpression (Sup. Fig. 1c).

## Enhanced $P2Y_2$ expression drives endothelial cells towards a proangiogenic phenotype

To further elucidate the role of $P2Y_2$ receptors in endothelial cells, we analyzed signaling downstream of $P2Y_2$ and VEGFR-2 activation. $P2Y_2$ overexpression impaired the ability of cells to proliferate in response to VEGF (Fig. 4a). Together with our gene array and functional assay data, this finding suggests that $P2Y_2$ overexpression results in constitutively active VEGF receptor signaling. Furthermore, we found significantly increased phosphorylation of ERK 1/2 in $P2Y_2^{OE}$-HUVEC compared to control cells (Fig. 4b). We then assessed whether $P2Y_2$ levels affect the cell-autonomous ability to form sprouts and vascular networks. Therefore, mosaic spheroids or cell-containing fibrin gels were generated by mixing endothelial cells expressing normal or elevated levels of $P2Y_2$ to determine which cell type is at the tip or participating in network formation. Control cells were retrovirally transduced with YFP or mCherry, while $P2Y_2$ overexpression was achieved by transduction with a fusion of $P2Y_2$ with YFP. We found that only $P2Y_2$-overexpressing cells sprouted or formed a primitive network in a competitive mosaic spheroid or fibrin matrix assay at baseline conditions, while control cells did not, suggesting that no paracrine factors are involved in this mechanism (Fig. 4c, d). Indeed, in tip cell or vascular network-favoring conditions (i.e., when paracrine factors such as VEGF are added or secreted by co-cultured MSC), control cells sprouted or formed a vascular network resulting in equal contribution of $P2Y_2^{OE}$ and CTRL cells to the sprouts or vascular networks (Sup. Fig. 2a, b). To determine if exogenous stimulation of $P2Y_2$ can influence sprouting, we treated EC spheroids with 100 µM UTP, another agonist of $P2Y_2$. This treatment did not affect sprouting parameters of CTRL-HUVEC under any condition tested (Fig. 4e, f). Instead, we found filopodia-like structures that emerged from spheroids when $P2Y_2^{OE}$-HUVEC were treated with UTP (Fig. 4e). These results suggest that increased $P2Y_2$ expression elicits this functional response to UTP. Furthermore, we found that constitutive phosphorylation of VEGFR-2 in unstimulated $P2Y_2^{OE}$-HUVEC was similar to that of VEGF-treated CTRL-HUVEC, which may explain why $P2Y_2$-overexpressing cells did not respond to VEGF treatments in functional assays (Fig. 4g). In addition, we observed that total VEGFR-2 protein levels were decreased in $P2Y_2^{OE}$-HUVEC (Fig. 4g). Based on our results from spheroid and fibrin matrix assays, we speculated that VEGF may induce the release of ATP to initiate autocrine $P2Y_2$ receptor signaling. In contrast to thrombin as positive control [34], VEGF stimulation of HUVEC did not result in measurable accumulation of extracellular ATP (Fig. 4h). In addition to $P2Y_2$, it has also been shown that endothelial cells abundantly express the purinergic receptor $P2Y_{11}$ which responds to the same ligand as $P2Y_2$ and couples to the same G protein [3]. However, overexpression of $P2Y_{11}$ in HUVEC did not influence sprouting in a spheroid sprouting assay (Sup. Fig. 2c, d) demonstrating the specific involvement of $P2Y_2$ in endothelial sprouting. Furthermore, we analyzed the influence of $P2Y_2$ overexpression on the mTOR and AKT pathways, and found rS6 and AKT phosphorylation unchanged in unstimulated cells (Sup. Fig. 2e, f). Together, these data suggest that $P2Y_2$ is required to facilitate VEGF-induced signaling and angiogenesis.

## Enhanced sprouting in response to $P2Y_2$ overexpression is VEGFR-2 dependent

To confirm the involvement of VEGFR-2 in spontaneous endothelial sprouting of $P2Y_2^{OE}$-HUVEC, we applied Apatinib, a selective VEGFR-2 inhibitor [35], to cells embedded in a fibrin matrix. Treatment of fibrin-embedded $P2Y_2^{OE}$-HUVEC with 1 µM Apatinib visibly impaired network formation after incubation of 1 week (Fig. 5a). The inhibition of VEGFR-2 significantly reduced the number of junctions, tubules and the total network length compared to DMSO-treated controls (Fig. 5b). These data indicate that signaling via VEGFR-2 is at least in part responsible for the observed effects despite its reduced expression in $P2Y_2^{OE}$-HUVEC. To elucidate if different Tie1 or Tie2 protein levels were responsible for the observed reduction of VEGFR-2 protein expression [36, 37] upon $P2Y_2$ overexpression, we performed flow cytometry analysis. Tie1 total, but not surface, protein levels were influenced by $P2Y_2$ overexpression in HUVEC (Fig. 5c). Interestingly, we observed that surface Tie2 levels were decreased, while total protein levels were not significantly affected by

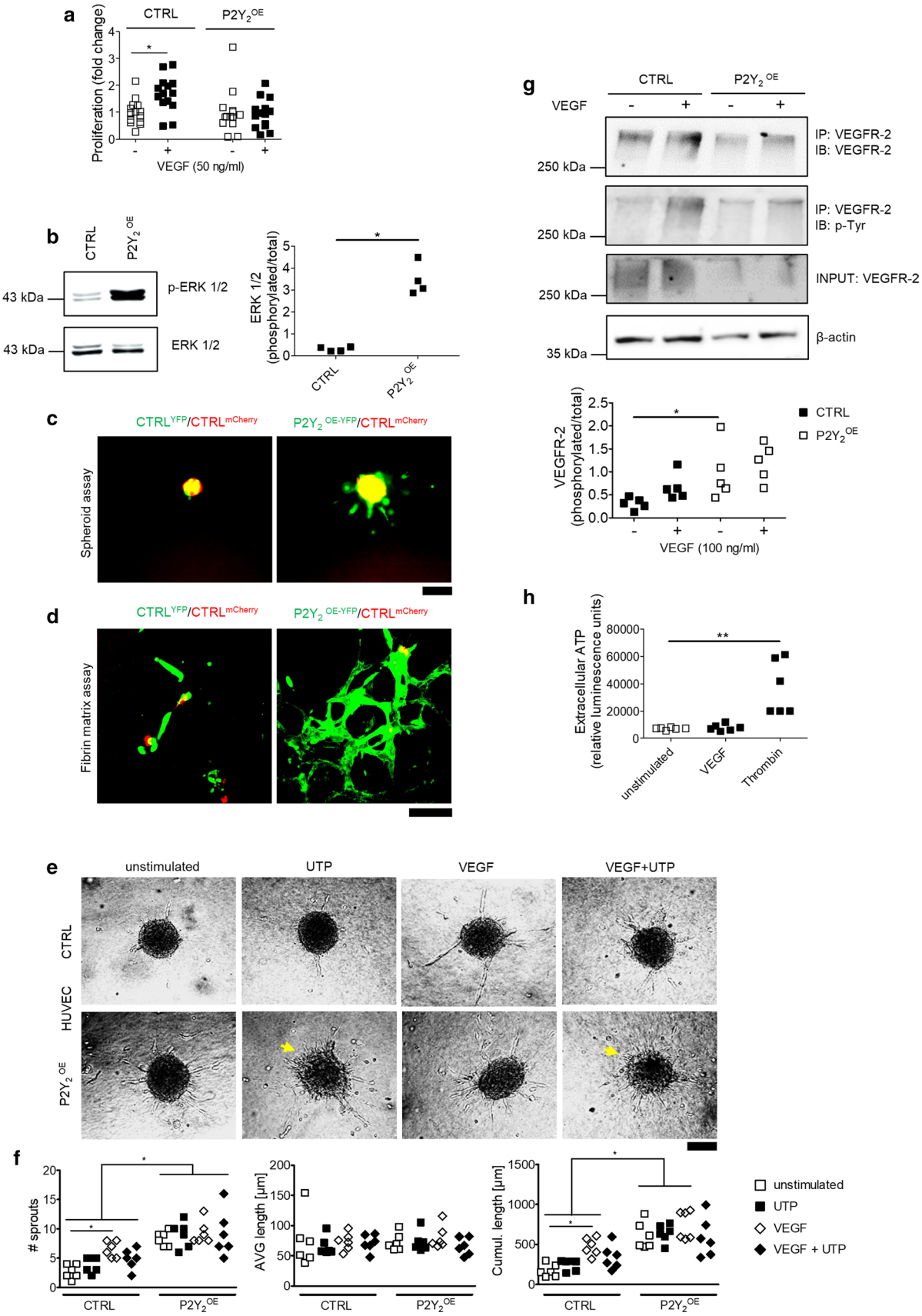
a
CTRL
P2Y2OE
Proliferation (fold change)
VEGF (50 ng/ml)
b
CTRL
P2Y2 OE
43 kDa
p-ERK 1/2
43 kDa
ERK 1/2
ERK 1/2 (phosphorylated/total)
c
CTRLYFP/CTRLmCherry
P2Y2 OE-YFP/CTRLmCherry
Spheroid assay
d
Fibrin matrix assay
e
unstimulated
UTP
VEGF
VEGF+UTP
CTRL
HUVEC
P2Y2 OE
f
# sprouts
AVG length [µm]
Cumul. length [µm]
unstimulated
UTP
VEGF
VEGF + UTP
g
VEGF
IP: VEGFR-2
IB: VEGFR-2
IP: VEGFR-2
IB: p-Tyr
INPUT: VEGFR-2
β-actin
250 kDa
35 kDa
VEGFR-2 (phosphorylated/total)
VEGF (100 ng/ml)
h
Extracellular ATP (relative luminescence units)
unstimulated
VEGF
Thrombin

◂**Fig. 4** Mechanisms of $P2Y_2$-induced vascularization. **a** VEGF failed to induce proliferation in cells overexpressing $P2Y_2$ as determined by BrdU assay. **b** Total cell lysates of control and $P2Y_2^{OE}$-HUVEC were subjected to immunoblotting with antibodies which recognize ERK 1/2 and p-ERK 1/2. Constitutive phosphorylation of ERK 1/2 could be measured in cells with enhanced $P2Y_2$ expression. Representative images of collagen mosaic spheroid (**c**) and fibrin matrix assays (**d**) where either vehicle-infected or $P2Y_2^{OE}$-HUVEC (both green) were co-embedded with vehicle-infected HUVEC (red). Mainly $P2Y_2^{OE}$ cells sprouted and formed a vascular network, while control cells did not, indicating an autocrine mechanism. **e** Representative images of UTP-stimulated spheroids, showing that no difference in sprouting upon stimulation could be observed in control cells, while appearance of filopodia-like structures emerged only from UTP-stimulated $P2Y_2^{OE}$-HUVEC (arrows). **f** Quantification of number of sprouts, average length, and cumulative length demonstrates that UTP stimulation had no effect on these sprouting parameters in either sample. **g** VEGFR-2 is constitutively phosphorylated in cells overexpressing $P2Y_2$ as determined by immunoprecipitation and blotting against phosphorylated tyrosine. A significant increase in tyrosine phosphorylation and decrease of total VEGFR-2 levels were observed upon $P2Y_2$ overexpression. **h** ATP content was determined in supernatants of stimulated HUVEC. VEGF 50 ng/ml does not trigger ATP release of HUVEC after 10 min of stimulation. Thrombin 1 U/ml was used as a positive control. Proliferation assay, ATP release experiment, normal and mosaic spheroid, and fibrin matrix assay data were obtained from two independent experiments using two donors. Immunoblots and immunoprecipitations were performed at least four times with protein lysates obtained from three HUVEC donors. * and ** indicate $p$ values of $<0.05$ and 0.01, respectively. Scale bars indicate 100 µm

enhanced $P2Y_2$ expression compared to controls, suggesting that Tie2 is internalized (Fig. 5d). Moreover, we did not find any differences in VEGFR-3 protein expression due to enhanced $P2Y_2$ expression (Sup. Fig. 2g).

### $P2Y_2$ influences sprouting and vasculogenesis in iPSC-ECFC

Endothelial cells may show differences in their phenotype depending on their organotypic origin in the human body [20]. To confirm that the influence of $P2Y_2$ overexpression is not specific to endothelial cells from umbilical veins, we overexpressed $P2Y_2$ in induced pluripotent stem cell-derived endothelial colony-forming cells (iPSC-ECFC). Flow cytometry analysis of endothelial surface proteins revealed that $P2Y_2$ regulates surface expression of CD34, VEGFR-2, and Tie2 in both HUVEC and iPSC-ECFC to similar extents (Fig. 6a). Quantification of fluorescence intensity showed that surface levels of VEGFR-2 were significantly decreased, while CD34 levels were significantly increased upon $P2Y_2$ overexpression (Fig. 6b). This is in line with our gene array and immunoblotting data (Figs. 3c–e, 4g). Surface protein levels of CD31, VE-Cadherin, CD73, and CD146 were either not influenced by $P2Y_2$ or only changed in one cell type. In addition, we found increased sprouting and vascular network formation upon $P2Y_2$ overexpression in the absence of an angiogenic stimulus in iPSC-ECFC (Fig. 6c–f). The increase in vascularization and sprouting upon enhanced $P2Y_2$ expression could, therefore, be recapitulated in these cells, suggesting that the observed effects are not limited to specific endothelial cell types. Taken together, these data confirm that enhanced $P2Y_2$ expression drives endothelial cells into a proangiogenic phenotype regardless of their origin.

## Discussion

Here, we report a novel role for the purinergic $P2Y_2$ receptor in the sprouting of endothelial cells. To determine the function of the $P2Y_2$ receptor during vascular growth, we forced overexpression of the receptor in ECs. Our results presented here show that sprouting and vascular network formation were significantly dependent on endothelial $P2Y_2$ expression and activity. Furthermore, our data indicate that ECs acquire a proangiogenic phenotype and lose their responsiveness to VEGF when the expression of $P2Y_2$ is enhanced. This is likely mediated by amplification of VEGFR-2 signaling and, thus, regulation of a major pathway of angiogenesis [13]. Indeed, inhibition of VEGFR-2 significantly impaired spontaneous vascular network formation induced by $P2Y_2$ overexpression in our experiments, proving that VEGFR-2 is involved in this process. Interestingly, it was previously reported that stimulation of ECs with uridine adenosine tetraphosphate ($Up_4A$) promotes angiogenesis in a 3D co-culture assay with ECs and pericytes as well as upregulation of several proangiogenic and purinergic genes including $P2Y_2$, $P2Y_4$, and $P2Y_6$ [39]. Consequently, the $Up_4A$-induced angiogenic activity could be blocked by a selective antagonist against $P2Y_6$, suggesting that other purinergic receptors could be at least in part involved in driving $Up_4A$-induced vascularization. To focus on the role of $P2Y_2$ in vascular growth, we additionally carried out functional assays using siRNA-mediated knockdown and AR-C118925, a small molecule antagonist targeting $P2Y_2$. It was previously demonstrated that this antagonist has at least 50-fold selectivity against all other human P2X and P2Y receptors, except for the $P2X_1$ and $P2X_3$ receptors, which were blocked by AR-C118925 at concentrations of about 1 µM [38]. However, $P2X_1$ and $P2X_3$ are barely detectable in endothelial cells, suggesting that these receptors may not interfere with the effects observed here [3]. Therefore, we chose to incorporate this highly selective antagonist in our assays to highlight the importance of $P2Y_2$ in endothelial cells.

$P2Y_2$ is known to be able to influence signaling of several tyrosine kinase receptors including epidermal growth factor receptor (EGFR), platelet-derived growth factor receptor

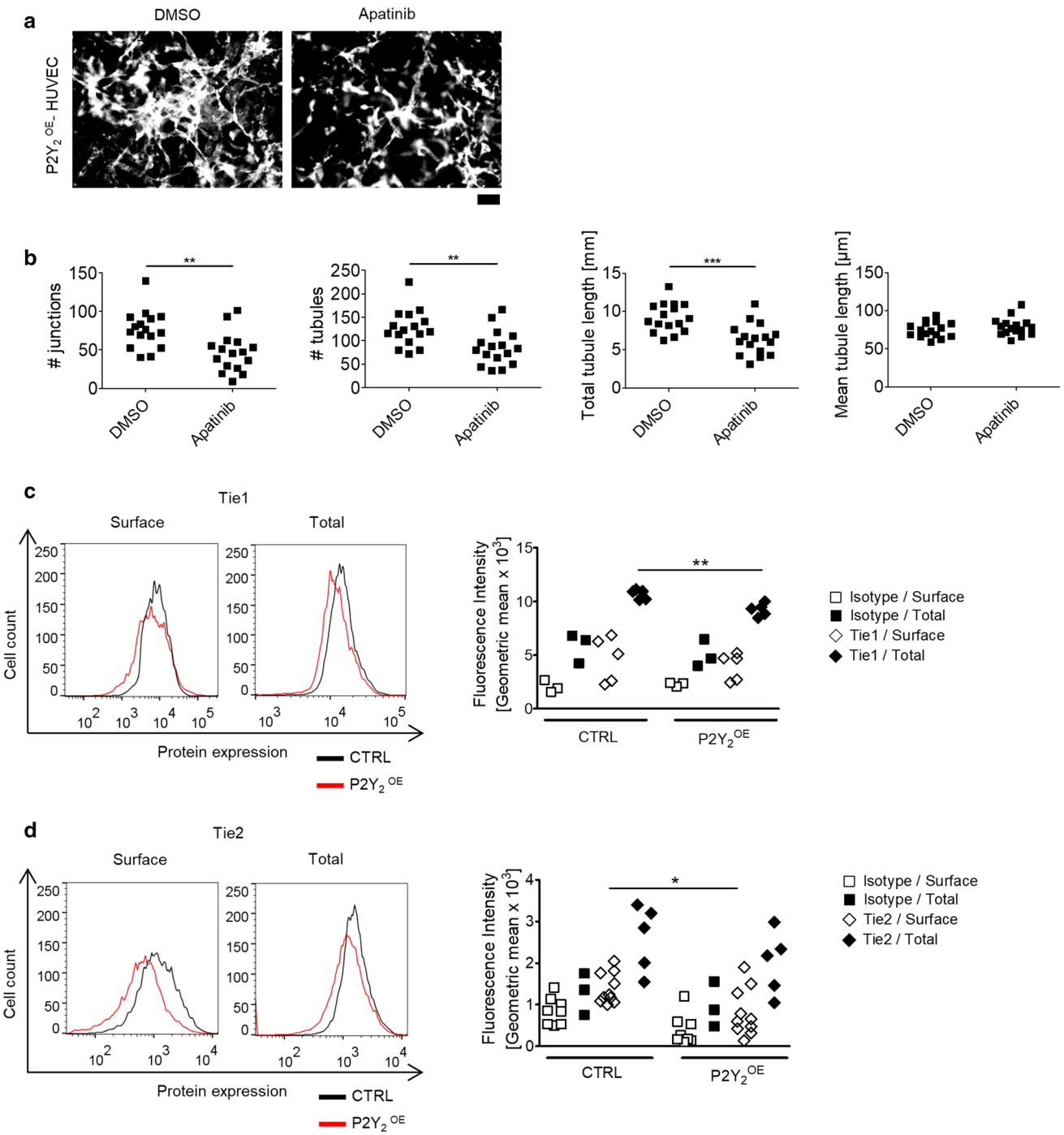


**Fig. 5** Role of VEGFR-2, Tie1 and Tie2 in $P2Y_2$-overexpressing cells. **a** Representative images of $P2Y_2^{OE}$-HUVEC embedded in fibrin matrices which were incubated with or without 1 µM Apatinib. **b** Analysis of vascular network parameters reveals that inhibition of VEGFR-2 significantly reduced the number of junctions, tubules, and the total network length but not the average tubule length of $P2Y_2$-overexpressing HUVEC. **c** Tie1 surface and total protein levels were measured using flow cytometry. No significant difference can be observed in Tie1 surface protein expression in $P2Y_2^{OE}$ cells, while total protein levels were significantly decreased. **d** Tie2 surface and total protein levels were measured using flow cytometry. Upon $P2Y_2$ overexpression, only surface but not total protein levels of Tie2 were significantly reduced. Graphs show data obtained from a minimum of three independent experiments using two different HUVEC donors. *, **, and *** indicate $p$ values of $<0.05$, 0.01, and 0.001, respectively. Scale bars indicate 100 µm

(PDGFR), and VEGFR-2 [8, 9, 12, 14, 40]. This receptor transactivation is mediated by Src-dependent activation of proline-rich tyrosine kinase 2 (Pyk2), a focal adhesion-related tyrosine kinase which is required for GPCR-mediated transactivation of receptor tyrosine kinases such as EGFR [12, 41]. In line with previously published reports, our data presented here demonstrate that interference with $P2Y_2$ receptor signaling can influence VEGFR-2 activity [8, 9, 14, 40]. Thus, constitutive interactions between these two receptors may allow $P2Y_2$ receptors to define functional cell responses to VEGF. However, the role of this transactivation mechanism has been unclear. Collectively, our observations here indicate that transactivation of VEGFR-2 by $P2Y_2$ is essential for vascular network formation and sprouting. Notably, $P2Y_2$ overexpression induces expression of several proangiogenic genes including CXCR4, CD34, and ANGPT2 in ECs. All three markers are reported to be enriched in tip cells [42–44]. This suggests that endothelial cells acquire a proangiogenic phenotype upon increased $P2Y_2$ expression, since tip cell-enriched genes seem to be co-regulated with $P2Y_2$.

We furthermore found increased CD34 and lower Tie2 surface protein levels, which represent another critical hallmark of angiogenic tip cells [44, 45]. Conversely, we detected decreased VEGFR-2 expression which has been observed in stalk cells only [46]. Nevertheless, the data presented here show lower expression of VEGFR-2 in $P2Y_2^{OE}$-HUVEC, yet higher phosphorylation which may act compensatory for reduced protein levels. Moreover, it has been shown that angiogenesis can occur upon inhibition of Notch even in the absence of VEGFR-2 if VEGFR-3 is upregulated [47]. Interestingly, our gene array analysis revealed an increased expression of VEGFR-3 in $P2Y_2^{OE}$-HUVEC which may substitute for lower VEGFR-2 expression levels to induce angiogenesis. However, we did not find significant differences in surface and total VEGFR-3 protein levels despite an observed increased expression in our gene array data. This indicates that VEGFR-3 may not be involved in the observed effects. In addition, our data here and previously published results suggest a correlation in protein expression between VEGFR-2 and Tie1 [36, 37]. One can speculate on a crosstalk of VEGF/VEGFR-2 and Ang/Tie signaling pathways upon $P2Y_2$ overexpression. VEGFR-2 internalization, recycling, and degradation can also be regulated by expression or junctional localization of VE-Cadherin [48]. Interestingly, $P2Y_2$ has been reported to be able to form a complex with VEGFR-2 and VE-Cadherin to regulate intracellular signaling factors such as Rac1 [9]. This complex formation could influence the junctional association of VE-Cadherin and thereby regulate VEGFR-2 levels. We have not detected any changes in the surface expression of VE-Cadherin, however, activation of $P2Y_2$ has been shown to induce phosphorylation of VE-Cadherin without influencing its expression [9].

Modulation of purinergic receptor expression has been shown to drive a variety of tasks in cells including cell differentiation and p38 MAPK activation as a response to injury [31–33]. Recently, it was reported that overexpression of $P2Y_2$ in human cardiac progenitor cells isolated from patients suffering from heart failure improved migration and proliferation and thereby the regenerative potential of these cells [49]. This is similar to our observations where forced expression of $P2Y_2$ in human ECs drives sprouting and vascular network formation, demonstrating that this receptor may perform similar functions in different tissues. Interestingly, we found that ERK 1/2 and VEGFR-2 were constitutively phosphorylated, suggesting that $P2Y_2$ may be continuously activated. Notably, reduced proliferation and increased phosphorylation of ERK 1/2 have been reported to be the characteristics of endothelial tip cells [46, 50].

The constitutive activation of $P2Y_2$ could be a result of permanent stimulation by a ligand or of increased basal receptor activity. It has been shown that a basal activity of $G_{q/11}$ signaling exists in endothelial cells and that modulation of this activity by influencing G protein expression facilitates VEGFR-2 phosphorylation [11]. This is in line with our data, demonstrating that $P2Y_2$ receptor overexpression induces VEGFR-2 activation in the absence of an exogenous ligand. Still, VEGF-induced release of $P2Y_2$ ligands may provide additional information on the connection of VEGFR-2 and $P2Y_2$, but we failed to detect any release of ATP in response to VEGF or any functional response to UTP stimulation unless $P2Y_2$ was overexpressed. This observation is supported by other reports, indicating that altered P2Y receptor expression affects essential EC functions [31–33]. Nevertheless, we cannot rule out the possibility that VEGF stimulation causes the release of small amounts of localized ATP and that autocrine stimulation of $P2Y_2$ receptors regulates functional HUVEC response to VEGF. Similar mechanisms have previously been reported to regulate pseudopodia protrusion of neutrophils during chemotaxis [2]. Release of ATP and autocrine signaling of $P2Y_2$ activates various mechanisms [2, 14], however, enhanced expression of $P2Y_2$ alone has been reported to be sufficient for activation of downstream signaling pathways [49]. This seems to be $P2Y_2$-specific as overexpression of another ATP-activated and $G_{q/11}$-coupled receptor $P2Y_{11}$, which is also reported to be abundantly expressed on ECs [3], does not induce any of the above-described effects. $P2Y_2$ carries unique features as it has equal binding affinities to its natural ligands ATP and UTP, however, β-arrestin recruitment and ERK 1/2 activation kinetics appear to be ligand-specific [19]. The question whether differential activation of $P2Y_2$ may be relevant in vascular growth remains and will be an interesting subject to be investigated in the future. Taken

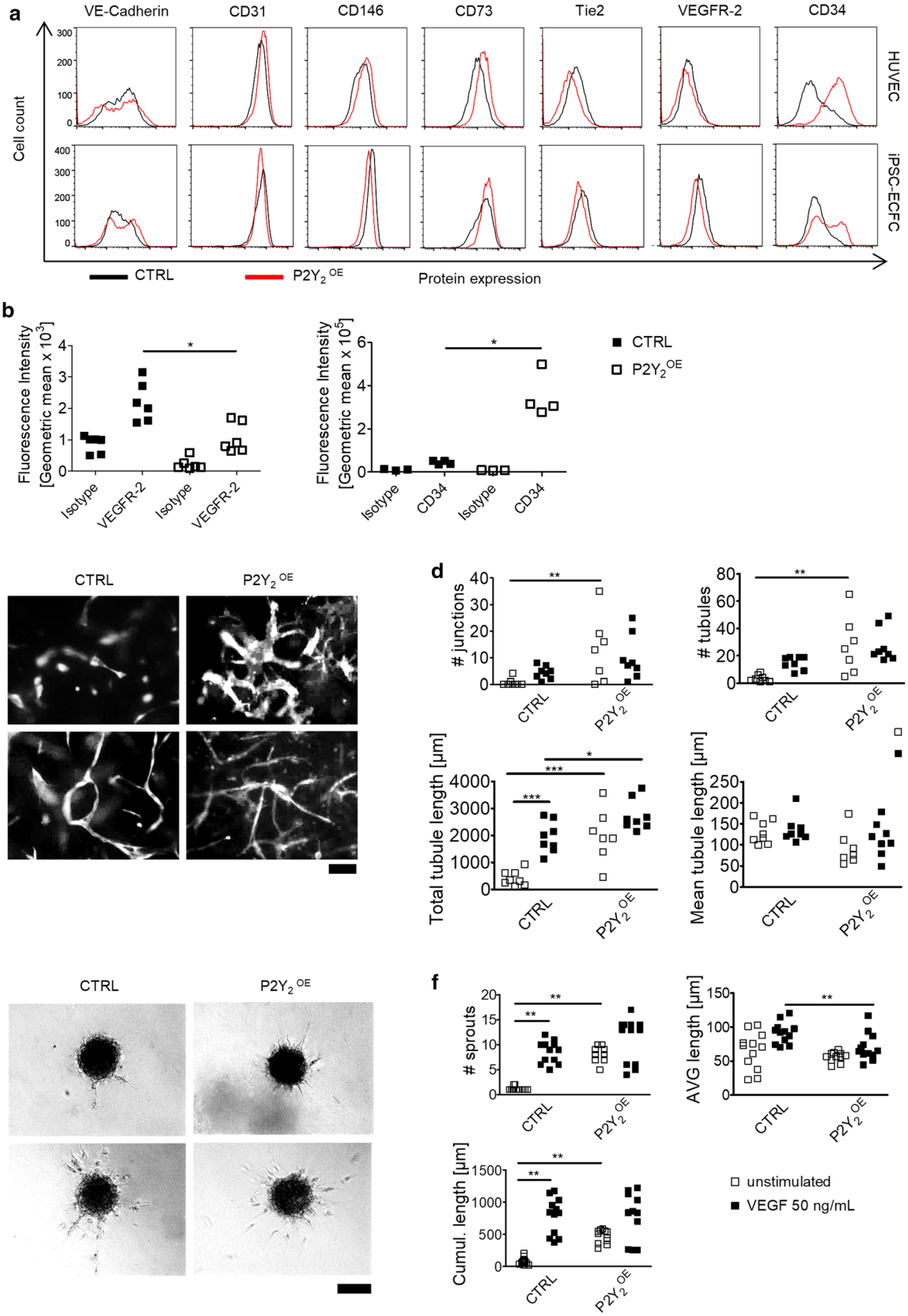
a
VE-Cadherin
CD31
CD146
CD73
Tie2
VEGFR-2
CD34
HUVEC
iPSC-ECFC
Cell count
CTRL
P2Y2 OE
Protein expression
b
Fluorescence Intensity [Geometric mean x 10^3]
Isotype
VEGFR-2
Fluorescence Intensity [Geometric mean x 10^5]
CD34
c
CTRL
P2Y2 OE
without MSC
with MSC
d
# junctions
# tubules
Total tubule length [µm]
Mean tubule length [µm]
without MSC
with MSC
e
unstimul.
VEGF
f
# sprouts
AVG length [µm]
Cumul. length [µm]
unstimulated
VEGF 50 ng/mL

◂**Fig. 6** $P2Y_2$ influences surface protein levels, sprouting, and vasculogenesis in iPSC-ECFC and HUVEC in vitro. **a** Flow cytometry measurements showed the influence of $P2Y_2$ overexpression on expression of selected surface markers in both HUVEC and iPSC-ECFC. **b** Analysis of geometric mean fluorescence (GMF) intensity reveals that surface protein levels of VEGFR-2 are decreased and of CD34 increased upon enhanced expression of $P2Y_2$ in HUVEC. **c** Representative images of iPSC-derived ECFC embedded in fibrin either alone or in co-culture with MSC. Overexpression of $P2Y_2$ in these cells results in formation of a primitive vascular network. **d** Analysis of vascular network parameters demonstrates a significant induction of network formation upon $P2Y_2$ overexpression. **e** Images of spheroids with iPSC-ECFC showing that $P2Y_2$ overexpression results in induction of sprouting. **f** Quantification of iPSC-ECFC spheroid images indicates a significant increase in sprouting potential upon $P2Y_2$ overexpression as determined by the number of sprouts, average length, and cumulative length per spheroid. Graphs show data obtained from a minimum of two independent experiments using different two HUVEC donors and one iPSC-ECFC donor. *, **, and *** indicate $p$ values of $<0.05$, 0.01, and 0.001, respectively. Scale bars indicate 100 µm

together, we conclude that $P2Y_2$-dependent vascular network formation occurs as a result of autocrine signaling. In addition, our data indicate that $P2Y_2$ overexpression in endothelial cells leads to loss of responsiveness to VEGF. Similar observations have been previously reported for endothelial colony-forming cells after stimulation with a non-selective P2 receptor agonist, which resulted in network formation on Matrigel at sub-optimal VEGF concentrations [6]. Nevertheless, the fact that inhibition or knockdown of $P2Y_2$ can significantly influence endothelial sprouting indicates that $P2Y_2$ does indeed play an essential role in angiogenesis. The blood vascular system is highly heterogeneous and fulfills different tissue-dependent tasks [51]. For instance, the majority of endothelial cells in a human body are found in microvascular structures, suggesting that human microvascular endothelial cells represent the most appealing source of ECs when studying wound healing and regeneration [20]. However, all of these endothelial cells from adult tissue represent a specialized cell type that may only reflect functions from the respective tissue [51]. Pluripotent cell-derived endothelial cells may offer a solution as they represent an unspecialized pan-endothelial cell type which can be used to study crucial functions in endothelial cell biology [52]. Here, we used iPSC-derived endothelial colony-forming cells which we believe represent an optimal source of unspecialized endothelial cells to confirm the role of $P2Y_2$ in angiogenesis. Indeed, we were able to reproduce our results from experiments with HUVEC in these cells, thereby proving that our described function of $P2Y_2$ may be similar throughout the entire endothelium.

Physiologically, $P2Y_2$ receptors expressed by the vascular endothelium have a vital role in vasorelaxation which was confirmed by $P2Y_2$ knockout mice experiments [1]. The trigger for vasodilation has been shown to be shear stress-induced ATP release from endothelial cells, resulting in autocrine activation of $P2Y_2$ leading to release of nitric oxide [17]. To our knowledge, we are the first to provide findings which suggest that $P2Y_2$ receptors fulfill a key function in vascular endothelial cells as crucial regulators of endothelial cell signaling during sprouting and vascular network formation in vitro. It is known that $P2Y_2$ can transactivate VEGFR-2 via Src in a VEGF-independent manner [13], which may represent a mechanistic explanation for the effects observed in this study. Alternatively, $P2Y_2$ has also been shown to co-localize with other endothelial cell surface molecules such as $\alpha_v\beta_3$ and $\alpha_v\beta_5$ integrins via its RGD motif to activate integrin signaling pathways or with VE-Cadherin which could lead to co-regulation of VEGFR-2 activity [9, 17]. Importantly, the data presented here demonstrate that $P2Y_2$ is a previously unrecognized component in the complex signaling network that regulates VEGF-induced angiogenesis. The fact that overexpression of $P2Y_2$ forces endothelial cells to acquire a tip cell phenotype implies that this receptor may be relevant as a therapeutic target in human vascular malignancies and pathologies.

**Acknowledgements** The authors thank Johannes Zipperle for isolating human platelets and Regina Grillari for providing Phoenix Ampho cells. This work was funded in part by the European Union's INTERREG V-A AT-CZ programme (ATCZ133), the City of Vienna Competence Team SignalTissue (#18-08) and by the Austrian Science Fund project SFB-F54. The funding sources have no influence on design and conduct of the study, collection, management, analysis and interpretation of the data, and preparation, review, or approval of the manuscript.

**Author contributions** SM performed retroviral infections, spheroid and fibrin matrix assays, flow cytometry, RT-PCR, and immunoprecipitations. SM and KL generated retroviral plasmids. CF and DS performed immunoblotting. SM and KP performed proliferation assays and analyzed iPSC-ECFC in flow cytometry. JP generated the gene array data. CS and JB analyzed gene array data. EP and CH supported the study by providing material. PS, WJ, and HR co-advised the project. SM and WH designed the figures and wrote the manuscript. WH was the lead advisor of this work. All authors read and approved the manuscript.

**Data and materials availability** Further information and requests for materials should be directed to the corresponding author Wolfgang Holnthoner. All raw files from mRNA analyses are available in the gene expression omnibus (GEO) under accession number GSE133795.

## Compliance with ethical standards

**Conflict of interest** The authors declare no competing interests.

## References

1. Burnstock G, Ralevic V (2014) Purinergic signaling and blood vessels in health and disease. Pharmacol Rev 66:102–192. https://doi.org/10.1124/pr.113.008029

2. Eltzschig HK, Sitkovsky MV, Robson SC (2012) Purinergic signaling during inflammation. N Engl J Med 367:2322–2333. https://doi.org/10.1056/NEJMra1205750
3. Wang L, Karlsson L, Moses S et al (2002) P2 receptor expression profiles in human vascular smooth muscle and endothelial cells. J Cardiovasc Pharmacol 40:841–853. https://doi.org/10.1097/00005344-200212000-00005
4. Jin H, Seo J, Eun SY et al (2014) P2Y2 R activation by nucleotides promotes skin wound-healing process. Exp Dermatol 23:480–485. https://doi.org/10.1111/exd.12440
5. Gidlöf O, Sathanoori R, Magistri M et al (2015) Extracellular uridine triphosphate and adenosine triphosphate attenuate endothelial inflammation through miR-22-mediated ICAM-1 inhibition. J Vasc Res 52:71–80. https://doi.org/10.1159/000431367
6. Rumjahn SM, Yokdang N, Baldwin KA et al (2009) Purinergic regulation of vascular endothelial growth factor signaling in angiogenesis. Br J Cancer 100:1465–1470. https://doi.org/10.1038/sj.bjc.6604998
7. Jacobson KA, Ivanov AA, de Castro S et al (2009) Development of selective agonists and antagonists of P2Y receptors. Purinergic Signal 5:75–89. https://doi.org/10.1007/s11302-008-9106-2
8. Seye CI, Yu N, González FA et al (2004) The P2Y2 nucleotide receptor mediates vascular cell adhesion molecule-1 expression through interaction with VEGF receptor-2 (KDR/Flk-1). J Biol Chem 279:35679–35686. https://doi.org/10.1074/jbc.M401799200
9. Liao Z, Cao C, Wang J et al (2014) The P2Y2 receptor interacts with VE-cadherin and VEGF receptor-2 to regulate Rac1 activity in endothelial cells. J Biomed Sci Eng 7:1105–1121. https://doi.org/10.4236/jbise.2014.714109
10. McEnaney RM, Shukla A, Madigan MC et al (2016) P2Y2 nucleotide receptor mediates arteriogenesis in a murine model of hind limb ischemia. J Vasc Surg 63:216–225. https://doi.org/10.1016/j.jvs.2014.06.112
11. Sivaraj KK, Li R, Albarran-Juarez J et al (2015) Endothelial Gαq/11 is required for VEGF-induced vascular permeability and angiogenesis. Cardiovasc Res 108:171–180. https://doi.org/10.1093/cvr/cvv216
12. Liu J, Liao Z, Camden J et al (2004) Src homology 3 binding sites in the P2Y2 nucleotide receptor interact with Src and regulate activities of Src, proline-rich tyrosine kinase 2, and growth factor receptors. J Biol Chem 279:8212–8218. https://doi.org/10.1074/jbc.M312230200
13. Erb L, Weisman GA (2015) Coupling of P2Y receptors to G proteins and other signaling pathways. Wiley Interdiscip Rev Membr Transp Signal 1:789–803. https://doi.org/10.1002/wmts.62
14. Wang S, Iring A, Strilic B et al (2015) P2Y2 and Gq/G11 control blood pressure by mediating endothelial mechanotransduction. J Clin Invest 125:3077–3086. https://doi.org/10.1172/JCI81067
15. Petzelbauer P, Bender JR, Wilson J, Pober JS (1993) Heterogeneity of dermal microvascular endothelial cell antigen expression and cytokine responsiveness in situ and in cell culture. J Immunol 151:5062–5072
16. Priglinger E, Maier J, Chaudary S et al (2018) Photobiomodulation of freshly isolated human adipose tissue-derived stromal vascular fraction cells by pulsed light-emitting diodes for direct clinical application. J Tissue Eng Regen Med 12:1352–1362. https://doi.org/10.1002/term.2665
17. Sathanoori R, Bryl-Gorecka P, Müller CE et al (2017) P2Y2 receptor modulates shear stress-induced cell alignment and actin stress fibers in human umbilical vein endothelial cells. Cell Mol Life Sci 74:731–746. https://doi.org/10.1007/s00018-016-2365-0
18. Weihs AM, Fuchs C, Teuschl AH et al (2014) Shock wave treatment enhances cell proliferation and improves wound healing by ATP release-coupled extracellular signal-regulated kinase (ERK) activation. J Biol Chem 289:27090–27104. https://doi.org/10.1074/jbc.M114.580936
19. Hoffmann C, Ziegler Reiner et al (2008) Agonist-selective, receptor-specific interaction of human P2Y receptors with beta-arrestin-1 and -2. J Biol Chem 283:30933–30941. https://doi.org/10.1074/jbc.M801472200
20. Knezevic L, Schaupper M, Mühleder S et al (2017) Engineering blood and lymphatic microvascular networks in fibrin matrices. Front Bioeng Biotechnol 5:1–12. https://doi.org/10.3389/fbioe.2017.00025
21. Hackethal J, Mühleder S, Hofer A et al (2017) An effective method of *Atelocollagen* type 1/3 isolation from human placenta and its in vitro characterization in two-dimensional and three-dimensional cell culture applications. Tissue Eng Part C Methods 23:274–285. https://doi.org/10.1089/ten.tec.2017.0016
22. Rohringer S, Holnthoner W, Hackl M et al (2014) Molecular and cellular effects of in vitro shockwave treatment on lymphatic endothelial cells. PLoS One 9:e114806. https://doi.org/10.1371/journal.pone.0114806
23. Sharov AA, Schlessinger D, Ko MSH (2015) ExAtlas: an interactive online tool for meta-analysis of gene expression data. J Bioinform Comput Biol 13:1550019. https://doi.org/10.1142/S0219720015500195
24. Qiagen IPA. https://www.qiagenbioinformatics.com/products/ingenuity-pathway-analysis. Accessed 4 July 2019
25. Liberzon A, Birger C, Thorvaldsdóttir H et al (2015) The molecular signatures database hallmark gene set collection. Cell Syst 1:417–425. https://doi.org/10.1016/j.cels.2015.12.004
26. Morpheus. https://software.broadinstitute.org/morpheus. Accessed 4 July 2019
27. Holnthoner W, Hohenegger K, Husa A-M et al (2015) Adipose-derived stem cells induce vascular tube formation of outgrowth endothelial cells in a fibrin matrix. J Tissue Eng Regen Med 9:127–136. https://doi.org/10.1002/term.1620
28. Hasenberg T, Mühleder S, Dotzler A et al (2015) Emulating human microcapillaries in a multi-organ-chip platform. J Biotechnol 216:1–10. https://doi.org/10.1016/j.jbiotec.2015.09.038
29. Wang L, Östberg O, Wihlborg AK et al (2003) Quantification of ADP and ATP receptor expression in human platelets. J Thromb Haemost 1:330–336. https://doi.org/10.1046/j.1538-7836.2003.00070.x
30. Sharma S, Rao A (2009) RNAi screening: tips and techniques. Nat Immunol 10:799–804. https://doi.org/10.1038/ni0809-799.RNAi
31. Du D, Zhou Z, Zhu L et al (2018) TNF-α suppresses osteogenic differentiation of MSCs by accelerating P2Y2 receptor in estrogen-deficiency induced osteoporosis. Bone. https://doi.org/10.1016/j.bone.2018.09.012
32. Shinozaki Y, Shibata K, Yoshida K et al (2017) Transformation of astrocytes to a neuroprotective phenotype by microglia via $P2Y_1$ Receptor downregulation. Cell Rep 19:1151–1164. https://doi.org/10.1016/j.celrep.2017.04.047
33. Kobayashi K, Yamanaka H, Fukuoka T et al (2008) P2Y12 receptor upregulation in activated microglia is a gateway of p38 signaling and neuropathic pain. J Neurosci 28:2892–2902. https://doi.org/10.1523/JNEUROSCI.5589-07.2008
34. Godecke S, Roderigo C, Rose CR et al (2012) Thrombin-induced ATP release from human umbilical vein endothelial cells. AJP Cell Physiol 302:C915–C923. https://doi.org/10.1152/ajpcell.00283.2010
35. Tian S, Quan H, Xie C et al (2011) YN968D1 is a novel and selective inhibitor of vascular endothelial growth factor receptor-2 tyrosine kinase with potent activity in vitro and in vivo. Cancer Sci 102:1374–1380. https://doi.org/10.1111/j.1349-7006.2011.01939.x
36. Savant S, La Porta S, Budnik A et al (2015) The orphan receptor Tie1 controls angiogenesis and vascular remodeling by

differentially regulating Tie2 in Tip and stalk cells. Cell Rep 12:1761–1773. https://doi.org/10.1016/j.celrep.2015.08.024
37. La Porta S, Roth L, Singhal M et al (2018) Endothelial Tie1-mediated angiogenesis and vascular abnormalization promote tumor progression and metastasis. J Clin Invest 128:834–845. https://doi.org/10.1172/JCI94674
38. Rafehi M, Burbiel JC, Attah IY et al (2017) Synthesis, characterization, and in vitro evaluation of the selective $P2Y_2$ receptor antagonist AR-C118925. Purinergic Signal 13:89–103. https://doi.org/10.1007/s11302-016-9542-3
39. Zhou Z, Chrifi I, Xu Y et al (2016) Uridine adenosine tetraphosphate acts as a proangiogenic factor in vitro through purinergic P2Y receptors. Am J Physiol Circ Physiol 311:H299–H309. https://doi.org/10.1152/ajpheart.00578.2015
40. Erb L, Weisman GA (2012) Coupling of P2Y receptors to G proteins and other signaling pathways. Wiley Interdiscip Rev Membr Transp Signal 1:789–803. https://doi.org/10.1002/wmts.62
41. Andreev J, Galisteo ML, Kranenburg O et al (2001) Src and Pyk2 mediate G-protein-coupled receptor activation of epidermal growth factor receptor (EGFR) but are not required for coupling to the mitogen-activated protein (MAP) kinase signaling cascade. J Biol Chem 276:20130–20135. https://doi.org/10.1074/jbc.M102307200
42. Strasser GA, Kaminker JS, Tessier-lavigne M, Dc W (2012) Microarray analysis of retinal endothelial tip cells identifies CXCR1 as a mediator of tip cell morphology and branching. Blood 115:5102–5110. https://doi.org/10.1182/blood-2009-07-230284
43. Toro R, Prahst C, Mathivet T et al (2010) Identification and functional analysis of endothelial tip cell enriched genes. Blood 116:4025–4033. https://doi.org/10.1182/blood-2010-02-270819
44. Siemerink MJ, Klaassen I, Vogels IMC et al (2012) CD34 marks angiogenic tip cells in human vascular endothelial cell cultures. Angiogenesis 15:151–163. https://doi.org/10.1007/s10456-011-9251-z
45. Felcht M, Luck R, Schering A et al (2012) Angiopoietin-2 differentially regulates angiogenesis through TIE2 and integrin signaling. J Clin Invest 122:1991–2005. https://doi.org/10.1172/JCI58832
46. Potente M, Gerhardt H, Carmeliet P (2011) Basic and therapeutic aspects of angiogenesis. Cell 146:873–887. https://doi.org/10.1016/j.cell.2011.08.039
47. Benedito R, Rocha SF, Woeste M et al (2012) Notch-dependent VEGFR3 upregulation allows angiogenesis without VEGF-VEGFR2 signalling. Nature 484:110–114. https://doi.org/10.1038/nature10908
48. Lampugnani MG, Orsenigo F, Gagliani MC et al (2006) Vascular endothelial cadherin controls VEGFR-2 internalization and signaling from intracellular compartments. J Cell Biol 174:593–604. https://doi.org/10.1083/jcb.200602080
49. Khalafalla FG, Greene S, Khan H et al (2017) P2Y2 nucleotide receptor prompts human cardiac progenitor cell activation by modulating hippo signaling. Circ Res 121:1224–1236
50. Rocha SF, Schiller M, Jing D et al (2014) Esm1 modulates endothelial tip cell behavior and vascular permeability by enhancing VEGF bioavailability. Circ Res 115:581–590. https://doi.org/10.1161/CIRCRESAHA.115.304718
51. Potente M, Mäkinen T (2017) Vascular heterogeneity and specialization in development and disease. Nat Rev Mol Cell Biol 18:477–494. https://doi.org/10.1038/nrm.2017.36
52. Jakobsson L, Franco CA, Bentley K et al (2010) Endothelial cells dynamically compete for the tip cell position during angiogenic sprouting. Nat Cell Biol 12:943–953. https://doi.org/10.1038/ncb2103